2140 *Biochemistry* **2010,** *49,* 2140–2149
DOI: 10.1021/bi901918f

BIOCHEMISTRY
including biophysical chemistry & molecular biology
Article

Amplitude of Pancreatic Lipase Lid Opening in Solution and Identification of Spin Label Conformational Subensembles by Combining Continuous Wave and Pulsed EPR Spectroscopy and Molecular Dynamics[†]

Sebastien Ranaldi,[‡] Valérie Belle,[‡] Mireille Woudstra,[‡] Raphael Bourgeas,[§] Bruno Guigliarelli,[‡] Philippe Roche,[§] Hervé Vezin,[⊥] Frédéric Carrière,*[,∥] and André Fournel*[,‡]

[‡]*CNRS Laboratoire de Bioénergétique et Ingénierie des Protéines, UPR 9036,* [§]*CNRS Laboratoire Interactions et Modulateurs de Réponses, FRE3083,* [∥]*CNRS Laboratoire d'Enzymologie Interfaciale et de Physiologie de la Lipolyse, UPR 9025, Institut de Microbiologie de la Méditerranée, Aix-Marseille Universités, Marseille, France, and* [⊥]*CNRS Laboratoire de Chimie Organique et Macromoléculaire, UMR 8009, Villeneuve d'Ascq, France*

Received November 8, 2009; Revised Manuscript Received February 3, 2010

ABSTRACT: The opening of the lid that controls the access to the active site of human pancreatic lipase (HPL) was measured from the magnetic interaction between two spin labels grafted on this enzyme. One spin label was introduced at a rigid position in HPL where an accessible cysteine residue (C181) naturally occurs. A second spin label was covalently bound to the mobile lid after introducing a cysteine residue at position 249 by site-directed mutagenesis. Double electron−electron resonance (DEER) experiments allowed the estimation of a distance of 19 ± 2 Å between the spin labels when bilabeled HPL was alone in a frozen solution, i.e., with the lid in the closed conformation. A magnetic interaction was however detected by continuous wave EPR experiments, suggesting that a fraction of bilabeled HPL contained spin labels separated by a shorter distance. These results could be interpreted by the presence of two conformational subensembles for the spin label lateral chain at position 249 when the lid was closed. The existence of these conformational subensembles was revealed by molecular dynamics experiments and confirmed by the simulation of the EPR spectrum. When the lid opening was induced by the addition of bile salts and colipase, a larger distance of 43 ± 2 Å between the two spin labels was estimated from DEER experiments. The distances measured between the spin labels grafted at positions 181 and 249 were in good agreement with those estimated from the known X-ray structures of HPL in the closed and open conformations, but for the first time, the amplitude of the lid opening was measured in solution or in a frozen solution in the presence of amphiphiles.

Lipases (triacylglycerol hydrolase, EC 3.1.1.3) are key enzymes in major physiological processes such as fat digestion and lipoprotein metabolism (*1*, *2*). These enzymes are also used in many industrial processes (biotransformation of oils and fats, synthesis of structured triacylglycerols, enantioselective reactions in organic synthesis) and products such as detergents for cleaning fat stains (*3*, *4*). Understanding their mechanism of action for then improving it is therefore a major challenge in biotechnology. One particular structural feature of lipases is the so-called "lid" that controls the access to the active site and the amphiphilic properties of these enzymes that are highly soluble in water but act at the surface of oil droplets (*5*). When the lid is "closed", the active site is not accessible to solvent, and the enzyme mainly presents a hydrophilic surface (*6*−*8*). When the lid is "open", the active site becomes accessible and functional, and a large hydrophobic surface is revealed at the surface of the protein surrounding the active site (*9*−*11*). This large hydrophobic surface becomes part of the active site, but it is also involved in the interaction of the lipase with the lipid−water interface. All of these structural characteristics have been revealed by X-ray crystallography since the last 20 years, the open conformations of lipases being often obtained by crystallization of lipase−inhibitor complexes and cocrystallization with detergents (*9*−*15*). Although these findings have been major breakthroughs in lipase studies, the structural behavior of lipases in solution, in the presence of detergent or organic solvents, or when they bind at the interface of two liquid phases remains still largely unknown. The use of NMR spectroscopy is not largely developed due to the high molecular masses of many lipases, and only a few lipases like cutinase (*16*, *17*) and *Pseudomonas mendocina* lipase (*18*) have been structurally characterized in solution by NMR.

The use of site-directed spin labeling (SDSL)[1] coupled to electron paramagnetic resonance spectroscopy (EPR) was however recently introduced for studying the conformational changes of the lid in human pancreatic lipase (HPL). By grafting a nitroxide spin label (MTSL) on the HPL lid at position 249, it was possible to identify specific EPR spectra of the spin label corresponding to the closed and open lid, and these spectra were later used for monitoring the HPL lid opening in solution (*19*). In particular, this study showed how an increasing concentration of

[†]The Ph.D. research of S.R. was supported by a grant from the French Ministery of Research and Education.

*To whom correspondence should be addressed. A.F.: tel, (33) 4 91 16 41 34; fax, (33) 4 91 71 58 57; e-mail, fournel@ifr88.cnrs-mrs.fr. F.C.: tel, (33) 4 91 16 41 34; fax, (33) 4 91 71 58 57; e-mail, carriere@ifr88.cnrs-mrs.fr.

[1]Abbreviations: CW, continuous wave; DEER, double electron−electron resonance; EPR, electron paramagnetic resonance spectroscopy; HPL, human pancreatic lipase; MD, molecular dynamics; MTSL, (1-oxy-2,2,5,5-tetramethyl-Δ^3-pyrroline-3-methyl)methanethiosulfonate; SDSL, site-directed spin labeling.

 Published on Web 02/05/2010

bile salts above their critical micellar concentration promotes the opening of the lid and how colipase, the specific HPL cofactor, plays a role in stabilizing the open conformation of the lid. An important finding was that the lid opening process was reversible as observed by decreasing the bile salt concentration under the micellar concentration. More recently, the structural changes induced in HPL by lowering the pH were investigated using a combined approach involving SDSL-EPR and Fourier transform infrared (ATR-FTIR) spectroscopy (*20*). A reversible opening of the lid was observed when the pH decreased from 6.5 to 3.0, giving an EPR spectrum similar to the one observed in the presence of bile salts and colipase. Below pH 3.0, ATR-FTIR measurements indicated that HPL had lost most of its secondary structure. In parallel, EPR studies were more precise in revealing a local unfolding in the vicinity of the active site, whereas the lid was found to resist to the global unfolding and to keep a stable structure. SDSL-EPR therefore appeared as a useful technique for studying both the mechanism of action and the stability of HPL.

The work reported in the present report is a further step forward in studying the HPL lid opening process by EPR. Using a double spin labeling strategy and pulsed EPR spectroscopy, the amplitude of the lid opening was estimated from double electron−electron resonance (DEER). Molecular dynamics led to the identification of two conformational subensembles for the spin label grafted on the lid, and the complete analysis of the magnetic interaction between this spin label and another one grafted at a rigid part of HPL confirmed this finding.

MATERIALS AND METHODS

Production of Recombinant HPL and HPL Mutant. All of the procedures used here have been previously described in detail in Belle et al. (*19*). The cDNA encoding HPL was previously obtained from human placenta mRNA using PCR methods (*21*). A 1411 bp *Bam*HI DNA fragment containing the entire HPL coding region was subcloned into the pGAPZB *Pichia pastoris* transfer vector (Invitrogen) downstream of the GAP constitutive promoter for further expression of HPL the yeast *P. pastoris*. Two HPL mutants (D249C and C181Y-D249C) were constructed using the PCR overlap extension technique as previously described, and they were also produced in *P. pastoris* after inserting their DNA into the pGAPZB vector. The wild-type *P. pastoris* strain X-33 was transformed by electroporation using linearized pGAPZB vectors containing either HPL or HPL mutant DNA. Cell cultures were then performed in 1 L Erlenmeyer flasks containing 200 mL of YPD medium without any zeocin, and the cell growth was stopped after 40 h in order to limit the proteolysis of the recombinant HPL (or mutant) secreted into the culture medium.

For the purification of HPL and HPL mutants, 2 L of yeast culture medium was collected, and the pure proteins were obtained after a single cation-exchange chromatography step on S-Sepharose gel (Pharmacia). The purified lipases were characterized by performing SDS−PAGE, N-terminal sequencing, and MALDI-TOF mass spectrometry analysis. Protein concentration in all samples used for EPR experiments was determined by amino acid composition analysis, and the enzyme specific activity was estimated from activity measurement performed with the pHstat technique and using tributyrin as substrate (*19*, *21*).

Spin Labeling Procedure. This procedure was described in previous reports (*19*, *20*). Since it was observed that free cysteines were oxidized in the recombinant lipase recovered from *Pichia* culture medium, the recombinant proteins were initially reduced with DTT prior to the spin labeling reaction with (1-oxy-2,2,5,5-tetramethyl-Δ^3-pyrroline-3-methyl)methanethiosulfonate (MTSL; Toronto Research Chemicals Inc., Toronto, Canada) for 1 h in ice. Upon performing the labeling and EPR measurements with the D249C HPL mutant for double spin labeling experiments, it appeared however that disulfide bridges might be slighty cleaved by DTT, and the resulting free cysteine might be also labeled with MTSL as suggested by a large background absorption revealed by EPR spectroscopy. In this case, the labeling procedure was therefore modified: the treatment by DTT was suppressed, and spin labeling with MTSL was performed for a longer period (4 h) at 4 °C. Four consecutive additions of MTSL at a 10 to 1 molar ratio versus HPL were required. When a single addition of MTSL at a 40 to 1 molar ratio was used, HPL was found to precipitate. All of the samples of HPL mutants treated with MTSL were checked by EPR spectroscopy, and those giving an EPR spectral shape typical of a labeled protein were pooled and concentrated at around 4 mg of HPL/mL (80 μM).

EPR Data Collection by CW EPR Spectroscopy. The spin-labeled HPL samples were injected into a quartz capillary tube with a useful volume of about 20 μL for both room and cryogenic temperature experiments, and the spin-labeled enzyme concentration ranged from 40 to 80 μM. Spectra were recorded at room temperature (296 K) on an ESP 300E Bruker spectrometer equipped with an ELEXSYS Super High Sensitivity resonator operating at 9.9 GHz. EPR spectra of the same samples were recorded at 150 K with an ELEXSYS E500 Bruker spectrometer fitted with an Oxford Instruments ESR 900 helium flow cryostat.

For room temperature experiment, the microwave power was set to 10 mW, and the magnetic field modulation frequency and amplitude were 100 kHz and 0.1 mT, respectively. At 150 K, the microwave power was set to 0.1 mW to avoid saturation of the signal, and the magnetic field modulation frequency and amplitude were 100 kHz and 0.4 mT, respectively.

EPR Data Collection by Pulsed EPR Spectroscopy. DEER experiments were achieved with a Bruker ELEXSYS E580 X band spectrometer using the standard MD5 dielectric resonator and equipped with an Oxford helium temperature regulation unit. All of the spectra were recorded at 70 ± 5 K. These experiments were performed using the four-pulse DEER sequence $(\pi/2)\nu_1-\tau_1-(\pi)\nu_1-\tau-(\pi)\nu_2-(\tau_1+\tau_2)-\tau-(\pi)\nu_1-\tau_2-$echo (*22*). The pump pulse (ν_2) length was set to 12 ns and applied at the maximum of the nitroxide spectrum corresponding to the $m_I = 0$ transition line, and its amplitude was optimized at the maximum of echo inversion. The observer pulses (ν_1) $\pi/2$ and π length were set respectively to 12 and 24 ns and positioned at a 72 MHz higher frequency corresponding to the transition $m_I = +1$. Signal processing was achieved using the DeerAnalysis2008 software package under Matlab (*23*). The signal was corrected by subtracting the unmodulated background echo decay by using a homogeneous three-dimensional spin distribution. The Tikhonov regularization was applied to the corrected dipolar evolution data set to obtain the distance distributions (*24*).

Simulation of the Room Temperature CW EPR Spectra. The EPRSIM-C software program used to simulate the EPR spectra was kindly provided by Dr. J. Strancar (University of Ljubljana, Slovenia). This program is based on the so-called motional-restricted fast-motion approximation and is described in detail in refs *25* and *26*. Five parameters were used to simulate the EPR spectra: an effective rotational correlation time τ, two angles, θ_0 and φ_0, which describe respectively the amplitude and the anisotropy of the spin label rotational motion within a cone,

a residual width (w), and a scalar parameter p_A which allows to adjust the value of the principal values of the hyperfine tensor describing the polarity of the environment of the probe. For a given polarity of the milieu, the shape of the EPR spectrum of a spin label grafted on a protein is governed by the partial averaging of its hyperfine and g tensors. This partial averaging is described by the values of the parameters τ, θ_0, and φ_0, the two last parameters being normalized by $\Omega = (\theta_0\varphi_0)/(\pi/2)^2$, representing the free rotational space which varies from zero (totally restricted movement) to 1 (unrestricted movement).

Simulation of the CW EPR Spectra at 150 K. The method used to simulate the EPR spectrum of a frozen solution of noninteracting nitroxide spin labels was previously described in Morin et al. (*27*). This home-built program was based on the diagonalization of the spin Hamiltonian describing the spin system (Zeeman and hyperfine interaction), the determination of the resonant magnetic field and the associated transition probabilities, and the evaluation of the line width of each transition line. For the present study, we added to the model the calculation of spin−spin interaction resulting from first-order dipolar interaction. The simulation was performed to estimate how the EPR spectrum of a frozen solution of spin-labeled HPL could be broadened by a fraction of strongly interacting spin labels (around 25%) compared to the EPR spectrum of a frozen solution containing 100% of noninteracting labels and not to precisely determine the distance between the closed spin labels. The calculated broadening was only arising from the first-order dipolar interaction, even when the spin labels were closed, which was a rough approximation since, in this later case, spin exchange and second-order dipolar interactions should be taken into account.

Molecular Dynamic Simulations. Molecular dynamics simulations were performed with the CHARMM19 extended atom force field (*28*). Spin label parameters and topology files were taken from a study by Dr. Piotr Fajer reported in ref *29*. Initial atomic coordinates of HPL in its closed conformation were retrieved from the Protein Data Bank (PDB ID 1N8S, HPL−colipase complex). All atoms corresponding to the colipase (chain C) were discarded. Serine residue 30B (numbering introduced by Winkler et al. (*7*)) was renumbered 31 and residues 31− 404 were renumbered accordingly (32−405). Residue Asp249 (Winkler's numbering) was replaced by a cysteine residue covalently linked to the MTSL nitroxide spin label using VMD and the psfgen software package (http://www.ks.uiuc.edu/Research/vmd/plugins/psfgen/). Missing coordinates were added with the hbuild procedure in CHARMM. A Monte Carlo search on the spin label torsion angles was used to define reasonable starting conformations for the spin label as described previously (*30*). The three lowest energy conformers were used as initial conformations. In addition, the three major χ_1,χ_2 rotamers observed in T4 lysozyme were used as initial structures (*31*) (Table 1). The structures were heated at 300 K (10 ps), equilibrated (75 ps), and subjected to free molecular dynamics (5 ns). Atoms beyond 30 Å of atom N1 of the spin label were fixed during the simulation. Molecular dynamics simulations were performed using a cutoff of 15 Å for nonbonded interaction. All bonds between hydrogens and heavy atoms were constrained with the SHAKE algorithm (*32*). An integration step of 1 fs was used. For each conformer, four independent trajectories were performed using different initial velocities.

Analyses were done with VMD (http://www.ks.uiuc.edu/Research/vmd/). Statistical analyses were performed with the R package.

Table 1: Initial χ_1 and χ_2 Dihedral Angles Used in MD Simulations

rotamer	χ_1	χ_2
1	305	120
2	60	230
3	292	53
t,p	180	60
t,m	180	270
m,m	280	310

RESULTS

Production and Biochemical Characterization of the Wild-Type (*wt*) *HPL and Mutants*. In addition to wt-HPL, two HPL mutants (D249C and C181Y-D249C) were produced in the yeast *P. pastoris* and further purified as previously reported in ref *19*. The wt-HPL was used for introducing a single spin label at position 181 where a free cysteine residue is naturally present and accessible to solvent. The HPL C181Y-D249C mutant was used for introducing a single spin label at position 249 within the HPL lid, after the substitution of C181 by a tyrosine residue. The HPL D249C mutant contained two accessible free cysteine residues at positions 181 and 249 for double spin labeling experiments. As previously done for wt-HPL and the HPL C181Y-D249C mutant (*19*), a biochemical characterization of the HPL D249C mutant was performed before the EPR experiments. N-Terminal sequencing confirmed that the signal peptide of this HPL mutant was correctly processed in the yeast and that no additional proteolytic cleavage occurred. MALDI-TOF analysis revealed a molecular mass of 51754 ± 36 Da similar to the mass previously measured for the glycosylated wt-HPL polypeptide. The specific activity on tributyrin of the spin-labeled HPL D249C mutant was found to be 6466 ± 1078 units/mg in the presence of bile salts (4 mM NaTDC) and colipase. This enzyme activity was similar to those previously recorded with HPL and the HPL C181Y-D249C mutant (*19*).

HPL Spin Labeling and Yield. The yield of protein spin labeling was estimated from the double integration of the CW EPR spectra of the labeled HPL recorded under nonsaturating conditions and at room temperature and compared with that given by a 3-carboxyproxyl sample of known concentration. Typical values obtained for the labeling yield were 70% spin label per protein molecule for a single spin label grafted at either position 181 (wt-HPL) or 249 (C181Y-D249C HPL mutant) in HPL and 140% when HPL was simultaneously labeled on both sites using the HPL D249C mutant. Assuming that each site was labeled with the same yield (70%), the proportion of bi-, mono-, and nonlabeled enzymes was estimated to be 49% (product of the labeling yield for both sites, 0.7 × 0.7), 42% (twice the product of the labeling yield for the first site and the nonlabeling proportion for the second site, 2 × 0.7 × 0.3), and 9% (product of the nonlabeling proportions for both sites, 0.3 × 0.3), respectively. Since the total HPL concentration was 80 μM, the respective concentrations of bi-, mono-, and nonlabeled HPL were estimated to be 39, 34, and 7 μM.

Observation of the Magnetic Interaction between the Two Spin Labels Grafted at Positions 181 and 249 (*Lid*) *of HPL*. (*A*) *Pulsed EPR Spectroscopy*. DEER experiments were performed with double spin-labeled HPL in order to measure the variations in the distance distributions during the lid opening process. Taking into account the low concentration of the bilabeled HPL (39 μM), DEER experiments data sets were recorded for 12 h at 70 K.

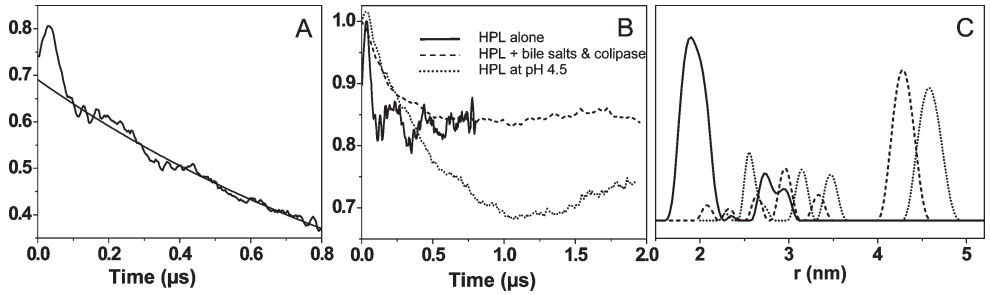

FIGURE 1: DEER experiments. (A) Experimental time domain data for bilabeled HPL alone in solution (black line) and homogeneous background function (gray line) used for correction of the unmodulated part of the spectrum. (B) Corrected experimental time domain data obtained in three conditions: HPL alone (solid line), in the presence of bile salts and colipase (dashed line), and at pH = 4.5 (dotted line). (C) Distance distributions obtained by Tikhonov regularization methods.

Figure 1A displays the experimental time domain data acquired with bilabeled HPL alone in solution and the homogeneous background function used to correct the unmodulated part of the dipolar echo decay (Figure 1B). The interspin distance distribution was extracted from the Tikhonov regularization of the corrected time domain spectrum. When HPL was alone in solution, a single distance distribution of 19 ± 2 Å was found (Figure 1C). The interspin distance distribution was shifted to 42 ± 2 Å in the presence of bile salts and colipase and to 46 ± 2 Å when the pH value was decreased from 6.5 to 4.5, these conditions being known for inducing the lid opening. These results indicated that the lid residue 249 was clearly pushed away from residue 181. The distance distributions obtained from Tikhonov regularization also showed minor peaks between 25 to 35 Å (Figure 1C). These peaks are generally considered as artifacts generated by the mathematical processing of data, but the time domain data contained a fast decaying component which was probably due to distances shorter than 42 Å between some spin labels. These minor peaks might therefore be due to minor intermediate conformations of the HPL lid leading to distances in between 19 Å (closed conformation) and 42 Å (open conformation) between the labels grafted at positions 181 and 249. There is also a possibility that these peaks resulted from a small fraction of unfolded HPL present in the sample as suggested by the simulation of the room temperature CW EPR spectra, but specific activity measurements performed prior to DEER experiments indicated that most HPL was correctly folded and the proportion of unfolded HPL is probably too small to be observed with DEER experiments.

(*B*) *CW EPR Spectroscopy*. Figure 2A′ displays the absorption spectrum at room temperature of the bilabeled HPL (positions 249 and 181) alone in solution compared to the spectrum of an equimolar mixture of C181 and C249 monolabeled HPL molecules. Strong magnetic interactions in the bilabeled HPL are revealed by the broadening of the absorption spectrum compared to the reference one. As the spectra were normalized to their integrated intensities, this broadening was characterized by a decrease of the central peak and by the presence of large outer wings. Since the slope of these enlarged outer wings was weak, the broadening was more visible in the absorption spectra (Figure 2A′) than in the first derivative ones (Figure 2A).

To check whether this broadening of the outer wings was due to a magnetic interaction of the spin labels, the EPR spectrum of the bilabeled HPL was recorded in the presence of colipase at a molar excess of 2 and 4 mM NaTDC to induce the opening of the HPL lid (65% open conformation (*19*)). In this case, the extension of the outer wings disappeared: the magnetic field range where the absorption takes place was nearly identical to the one observed in the absorption spectrum of an equimolar mixture of C181 and C249 monolabeled HPL molecules in the closed conformation (Figure 2A′,B′).

These results show that the opening of the lid dramatically weakens the strong intramolecular magnetic interaction between spin labels observed when the HPL is in its closed conformation. Moreover, the large extension of the outer wings observed for the bilabeled HPL in the closed conformation indicates that the interspin distance is probably lower than 10 Å.

It is worth noting that when the lid opens, the variations of the shapes observed for the low- and high-field peaks are largely due to the influence of the variation of the mobility of the spin label grafted at position 249 when this opening takes place and moderately to the interaction between spin labels (Figure 2B′).

In order to detect only the influence of the magnetic interaction between spin labels, we suppressed the influence of mobility of these labels by recording EPR spectra of frozen solutions (150 K) of the bilabeled HPL in the closed and open conformations (Figure 2C′). A broadening of the absorption spectrum was still observed for HPL in the closed conformation compared to the open one. In the presence of NaTDC and colipase, the absorption spectrum of the bilabeled HPL was found to be nearly identical to those recorded with monolabeled HPL at either position 181 or 249 (data not shown). No significant magnetic interaction between the two spin labels was therefore detectable in the presence of NaTDC and colipase under cryogenic conditions.

Simulation of the Room Temperature CW EPR Spectra of the Spin Label Grafted on the HPL Lid. The simulation of the CW EPR spectrum of the spin label grafted at position 249 on the HPL lid was first performed for the enzyme alone in solution, i.e., with the lid in the closed conformation (*19*). The best fit to the experimental EPR spectrum was obtained with three components (Figure 3A and Table 2). Two narrow-shaped components corresponding to spin labels with moderate mobility were found to largely contribute to the overall spectrum in nearly equal proportions (40% and 50%, respectively). It is worth noting that the term "mobility" takes into account both the rate of the rotational motion (described by τ) and the geometrical restrictions defining the anisotropy of the rotational motion (described by Ω). A third component corresponding to a spin label having a minor contribution to the overall spectrum (10%) was also required to obtain the best fit. This might result from the fact that some spin labels might be grafted on a small fraction of unfolded HPL that could not be detected by the classical biochemical analysis (enzyme activity and protein concentration

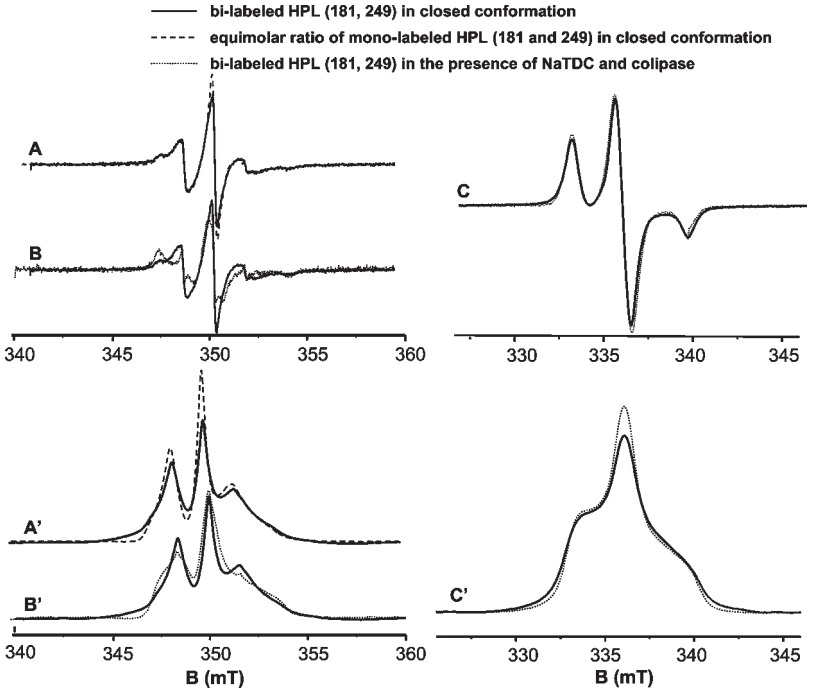

FIGURE 2: CW EPR spectra of mono- and bilabeled HPL. Panels A, B, and C are showing original derivative spectra measured with field modulation and panels A′, B′, and C′ the corresponding absorption spectra obtained from the integration of the conventional derivative spectra. (A, A′) Comparison of the spectra of the bilabeled HPL (positions 181 and 249; solid line) and the sum of the monolabeled HPL in equivalent proportion in the closed conformation (dotted line), recorded at room temperature. (B, B′) Comparison of the spectra of the bilabeled HPL alone in solution (closed conformation; solid line) and in the presence of 4 mM bile salts and colipase at a molar excess of 2 (65% open conformation; dotted line), recorded at room temperature. (C, C′) Comparison of the spectra recorded at 150 K for the bilabeled HPL alone in solution (solid line) and in the presence of bile salts and colipase (dotted line). All spectra have been normalized to their integrated intensities.

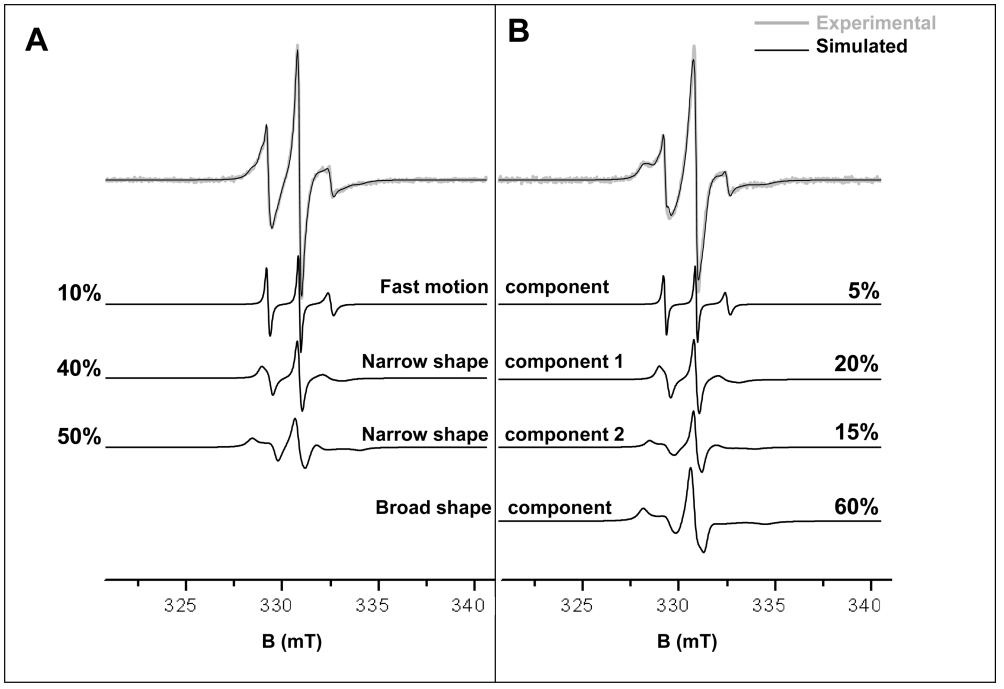

FIGURE 3: Simulation of EPR spectra and decomposition in individual components for the HPL alone in solution (A) and in the presence of 4 mM NaTDC and a molar excess of colipase (B). Simulations of the spectra were performed using the EPRSIM-C software program (*25*). See Table 2 for the parameters describing each spectral component.

assays) used for monitoring the production of HPL samples. The presence of residual free radical was excluded since the mobility would have been much higher.

The simulation of the CW EPR spectrum of the spin label grafted at position 249 on the HPL lid was then performed for the enzyme in the presence of micellar concentration of bile salts (4 mM NaTDC) and colipase in molar excess. Under these conditions, it was previously shown that the respective proportions of HPL molecules with the lid in the closed and open conformations were 35% and 65%, respectively (*19*). Upon

Table 2: Parameters Extracted from the Simulation of the CW EPR Spectra

		simulation parameters			
		τ_c (ns)	Ω	θ_0	φ_0
fast motion component		0.20	0.92	1.57	1.45
closed HPL alone in solution	narrow shape component 1	2.70	0.80	1.35	1.45
	narrow shape component 2	2.80	0.47	0.90	1.30
open HPL in the presence of 4 mM NaTDC and a molar excess of 2 in colipase	narrow shape component 1	2.60	0.74	1.30	1.40
	narrow shape component 2	2.80	0.44	0.90	1.20
	broad shape component	2.85	0.22	0.60	0.90

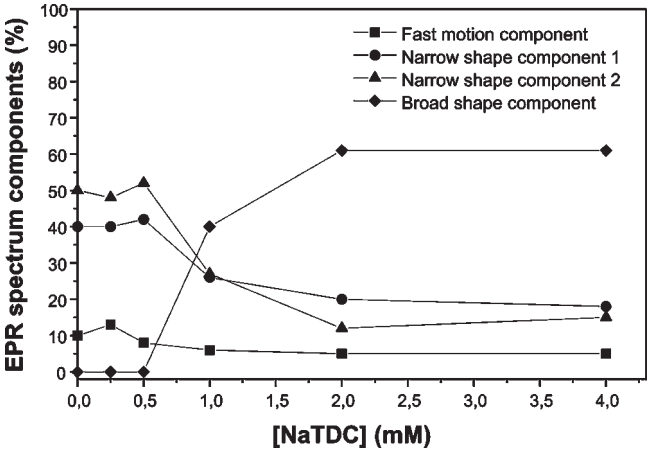

FIGURE 4: Variations with bile salt concentration in the proportion of the individual spectral components obtained by simulation of the experimental spectra.

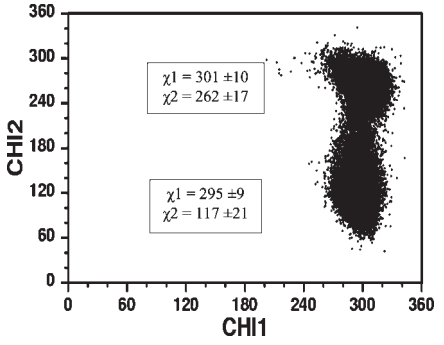

FIGURE 5: Populations of χ_1 and χ_2 dihedral angles obtained by molecular dynamics for the side chain of cysteine modified by MTSL at position 249 of the closed HPL.

simulation of the overall EPR spectrum, four components were required to obtain the best fit (Figure 3B and Table 2). As for the previous case, a minor fast motion component (5%) needed to be introduced. A major broad-shaped component was found to contribute to 60% of the whole spectrum. This component corresponds to the fraction of the HPL in the open conformation, according to our previous study (*19*). Two narrow-shaped components were found to represent 35% of the whole spectrum, and their shapes were nearly identical to those obtained for the EPR spectrum corresponding to HPL with the lid in its closed conformation (Figure 3 and Table 2). These two proportions (60% broad and 35% narrow shapes, respectively) were therefore highly similar to those estimated directly from the experimental spectrum. Hence, both the spectral shapes and the proportion of the two narrow-shaped components indicated that they result from spin labels in the enzyme fraction that has remained with the lid in the closed conformation. These two narrow components might be attributed to the presence of two conformational subensembles of the spin label side chain at position 249 when the lid is closed. On the other hand, the appearance of only one broad-shaped component upon lid opening suggests that only one conformational subensemble is present in the open HPL.

We simulated the EPR spectra obtained when the conformation of the HPL lid was progressively shifted from the closed to the open one using NaTDC in the presence of colipase (see experimental results in ref *19*). The largest proportion of the open conformation that could be obtained was 65%. The variations in each spectral component plotted as a function of NaTDC concentration are shown in Figure 4. The proportions of the two narrow-shaped components were found to decrease simultaneously when the NaTDC concentration and therefore the proportion of HPL in the open conformation were increased. Conversely, the broad-shaped component appeared and increased with NaTDC concentration above 0.5 mM, with a maximum level reached when the proportions of the two narrow-shaped components were the lowest. These results therefore suggest a transition of the spin labels from two distinct environments with moderate mobility to a single environment with low mobility.

Molecular Dynamics of the Cysteine Lateral Chain Labeled with MTSL at Position 249 of the Closed HPL. The root-mean-square deviations (rmsd) for Cα atoms during the time course of the different simulations were between 0.5 and 1 Å, indicating that the simulated system was stable. The X-ray crystallography structure of HPL has shown that the lid thermal factor is high (*7*, *10*), and as expected the root-mean-square fluctuation (rmsf) of the backbone revealed that the spin label is located in a flexible region. MD simulations showed two major conformational subensembles of the labeled C249 side chain characterized by their χ_1 and χ_2 dihedral angles (Figure 5). The average observed value for χ_1 was around 300° for both conformations whereas values of 120° and 260° were found for χ_2. Multimodal distributions were also observed for the other χ_3, χ_4, and χ_5 angles of the spin label in the MD simulations (data not shown). Two representative conformations were extracted from these results to estimate distances between spin labels from 3D models shown in Figure 6.

DISCUSSION

Evidence for Distinct Conformational Subensembles of the Spin Label Grafted to the Closed Lid of HPL. Experiments performed with concentrated samples (>100 μM) of HPL spin labeled at position 249 revealed that the EPR spectrum

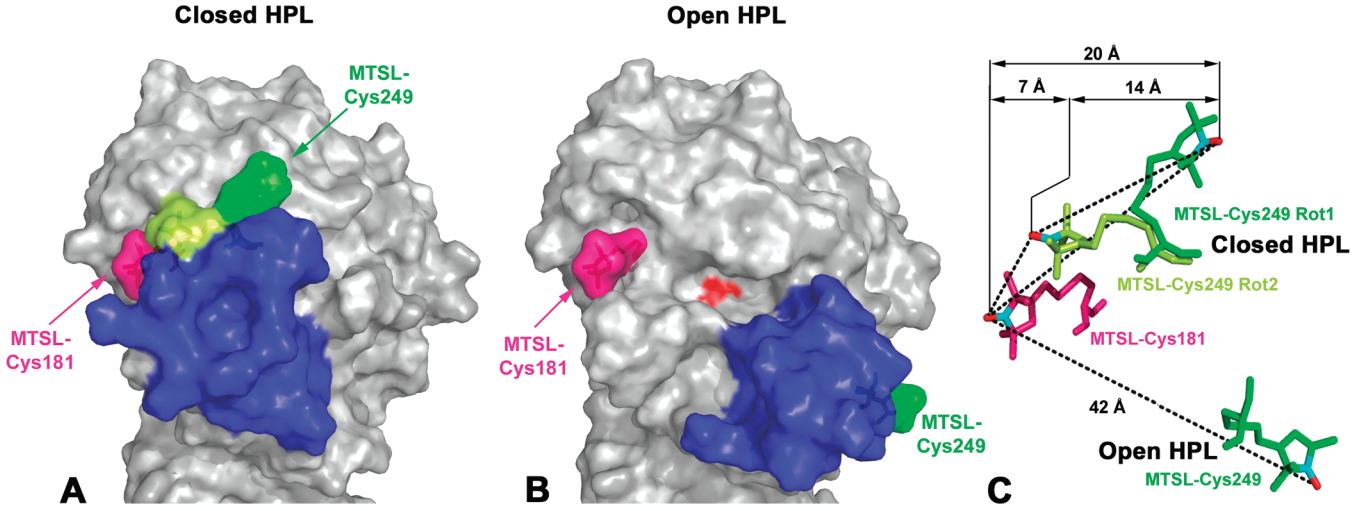

FIGURE 6: Structural modeling of spin labels grafted to cysteine residues in HPL. (A) Surface representation of HPL with the lid (blue surface) in the closed conformation, (B) surface representation of HPL with the lid (blue surface) in the open conformation and the active site accessible to solvent (the surface of the active site serine residue is colored in red, and (C) distances between the oxygen atoms of spin labels measured in silico. Atomic coordinates of HPL in its closed and open conformations were retrieved from the Protein Data Bank (closed HPL, PDB ID 1N8S; open HPL, 1LPB). The spin label at position 181 (MTSL-CYS181) is shown in magenta color in both closed and open HPL. The spin label at position 249 is shown in three different situations: two rotamers representative of the conformational subensembles observed by MD when the lid is closed (MTSL-CYS249-Rot1 colored in green and MTSL-CYS249-Rot2 colored in yellow, panels A and C) and the single conformation modeled in the open structure of HPL (MTSL-CYS249 colored in green in panels B and C). This figure was generated using the PyMOL software program (http://www.pymol.org/).

corresponding to the closed conformation of the HPL lid was in fact composite. The simulation of this EPR spectrum required the introduction of two narrow-shaped components of nearly equal weights. These components correspond to distinct environments and moderate mobilities of the nitroxide spin label (Figure 3A and Table 2) that could result from either two different closed conformations of the lid or the existence of two distinct side chain conformational subensembles in a single closed conformation of the lid.

Concerning the first hypothesis, only one closed conformation of the HPL lid was observed so far by X-ray crystallography (*7*, *33*). An intermediate conformation between the closed (inactive) and open (fully activated) conformations of *Thermomyces* (*Humicola*) *lanuginosa* lipase was however observed (*34*). This intermediate conformation, in which the active site remained not accessible to the solvent, was considered as a step occurring in the first phases of the lipase activation (opening of the lid). Discrete structural changes were observed upon the transition from the closed to this intermediate conformation, such as the isomerization of a disulfide bond synchronized with the flipping of an arginine located in the lid's proximal hinge. Changes of this kind might also occur in HPL and affect the conformation of amino acid side chains in the lid without a full opening of the active site. A spin label grafted to a residue in the lid might then be split into distinct populations showing slightly different but still moderate mobilities, whereas the drastic conformational change that occurs when the lid opens leads to the quasi immobilization of the spin label grafted at position 249 (Figure 3B). As suggested for the lipase of *T. lanuginosa*, an intermediate but still closed conformation of the HPL lid might then evolve toward the open one in a more favorable way than the closed conformation.

The second hypothesis of two distinct side chain conformational subensembles existing in a single closed conformation of HPL was supported by molecular dynamics experiments, showing the existence of two major conformational subensembles for the C249 side chain chemically modified by MTSL (Figures 5 and 6 and Table 1). Using the notation of Lowell (*35*), these two conformational subensembles adopt a m120 state ($\chi_1 = -60°$; $\chi_2 = 120°$) and a m-100 state ($\chi_1 = -60°$; $\chi_2 = -100°$). Since MD were performed at 300 K, one could argue that the distribution within the subensemble may not reflect exactly the population ensemble due to insufficient conformation sampling (*36*, *37*). It has been shown, however, that the use of stochastic dynamics simulations as was performed in this study leads to better conformation sampling (*38*). In addition, the use of CMAP correction with the CHARMM force field improves the treatment of Φ and ψ dihedral angles (*39*). Two conformational subensembles of spin-labeled cysteine lateral chains have been previously observed by X-ray crystallography for T4 lysozyme (*31*, *40*−*42*) and predicted by molecular dynamics for RalGDS-like protein 2 (*43*). The corresponding EPR spectra were found to contain two components which were attributed to these conformational subensembles in both spin-labeled T4 lysozyme (*40*) and RalGDS-like protein 2 (*43*): the conversion time between the two conformational subensembles, governed by the high energy activation of the disulfide bond $S\gamma-S_\delta$ present in the side chain, was sufficiently slow to observe the two components with X band EPR spectroscopy. In T4 lysozyme, these conformational subensembles were always observed in exposed α-helices. In the present study, the spin label conformational subensembles were also identified for an exposed position (residue 249) located in an α-helical region when the HPL lid is in the closed conformation: the short α-helix sitting on the top of the active site entrance (*7*). When the lid opens, residue 249 is still exposed to solvent but becomes located in a turn between two novel α-helices, and we observed only one component for the spin label in this case. The simultaneous disappearance of the two narrow-shaped components when the lid opens (Figure 4) is a strong support for this second hypothesis versus the existence of two distinct conformations of the closed lid.

Distance Estimation between Spin Labels and Amplitude of the Lid Opening in HPL. Distance distributions between the labels grafted on the lid and at position 181 were estimated from

the analysis of their dipolar interaction by the way of the double electron−electron resonance (DEER) method implemented on a pulsed EPR spectrometer. An estimation of these distances was also performed using the CW EPR spectra obtained at room temperature and 150 K.

Since we have two populations of the spin labels at position 249 in the closed conformation of the enzyme and one population for the same spin label in the open conformation (Figure 6), it was expected that we should measure two distances between nitroxides at position 181 (one population) and position 249 (two populations) when HPL is in the closed conformation, and three distances for the sample containing a mixture of closed (35%) and open (65%) conformations of the enzyme in the presence of bile salts and colipase.

With the DEER measurements and HPL in the closed conformation, a single mean distance of 19 ± 2 Å between the spin labels was however measured (Figure 1). The two distances expected between the two populations of the spin label at position 249 and the spin label at position 181 might therefore be either equal or more probably one of the two distances might be lower than 15 Å, the smallest value that can be measured by this technique. Indeed, the broadening observed on the CW EPR spectrum indicated that a fraction of double spin-labeled HPL in the closed conformation contained spin labels involved in a strong magnetic interaction and therefore separated by a short distance (Figure 2). These results are well supported by the structural modeling of spin-labeled HPL using known 3D structures and the results of molecular dynamics, with two values of 20 and 7 Å estimated for the distances between the nitroxide at position 181 and the two representative conformational subensembles at position 249 (Figure 6A,C). The modeling of the side chain of the spin-labeled C181 residue did not require MD simulations since its conformation was found to be drastically constrained by the local environment, and it was adjusted manually.

When the lid opening was induced by bile salts and colipase, the CW EPR spectrum at room temperature did not show this strong interaction anymore (Figure 2B′). Since the concentration of bilabeled HPL was 39 μM and 65% of HPL was in the open conformation, the concentration of the bilabeled and open HPL contributing to the CW EPR spectrum was estimated to be 25 μM. The absence of detectable interaction between spin labels was therefore not due to low concentrations of bilabeled HPL but was merely due to a distance greater than 20 Å between the spin labels, the limit value for detecting magnetic interaction with CW EPR. This is consistent with X-ray crystallography data showing that the maximum value of Cα displacement was 28−30 Å for the lid residues upon opening (Figure 6A,B). On the other hand, since 35% of HPL remained with the lid in the closed conformation, one could expect that some strong interaction between spin labels might still be seen from the CW EPR spectrum. The concentration of bilabeled HPL remaining in the closed conformation was however estimated to be only 14 μM, and only one spin label conformational subensemble at position 249 could give a strong interaction with the spin label at position 181. Since the two spin label conformational subensembles at position 249 were estimated to be in equal proportions (Figures 4B and 5), the concentration of bilabeled and closed HPL that could give a strong interaction between spin labels (distance lower than 10 Å) was found to be close to 7 μM (i.e., 9.4% of spin-labeled HPL). The overall EPR spectrum was therefore resulting from more than 90% of noninteracting or weakly interacting spin labels, and it is not surprising that no strong magnetic interaction was detected from the CW EPR spectrum. Concerning the spectra recorded at 150 K (Figure 2C′), we checked that the spectrum recorded for HPL in the presence of bile salts and colipase was not broadened by dipolar interaction (data not shown). For HPL alone in a frozen solution at 150 K (i.e., in the closed conformation of HPL), the observation of a broadening of the EPR spectrum was thus attributed to a magnetic interaction arising from a fraction of bilabeled molecules with two closed radicals. This broadening was however moderate (Figure 2C′). Since the EPR spectrum resulted from the contribution of 34 μM monolabeled HPL molecules (i.e., 47%), 19.5 μM bilabeled HPL molecules (i.e., 26.5%) with spin labels separated by a mean distance of 19 Å, and 19.5 μM bilabeled HPL molecules (i.e., 26.5%) with spin labels separated by a distance of about 8−10 Å, it was checked whether 26.5% of the spin-labeled HPL molecules with closed and strongly interacting spin labels could have such a moderate effect on the overall EPR spectrum of spin-labeled HPL in a frozen solution, as compared to the EPR spectrum of a frozen solution containing 100% of noninteracting labels. For this purpose, the EPR spectrum of the frozen solution was simulated (see Materials and Methods section) using the above proportions of monolabeled and bilabeled HPL molecules and, in this latter case, interspin label distances equal to 19 and 8−10 Å. This simulation was found to be consistent with the experimental spectrum (result not shown).

The HPL lid opening by bile salts was confirmed by the DEER experiments performed with pulsed EPR. A single mean value of 42 ± 2 Å was estimated for the distance between the spin labels grafted at position 181 and on the lid at position 249 (Figure 1). The distance between these nitroxides was therefore increased by a factor of 2 in the presence of bile salts and colipase. Again, these results are well supported by the structural modeling of spin-labeled HPL using the known 3D structure of HPL in the open conformation, with a value of 42 Å estimated for the distance between the nitroxides at positions 181 and 249 (Figure 6B,C). The various conformations tested for the side chain of the spin label at position 249 all gave distances in the 40 Å range and lower distances appeared to be impossible since this spin label was on the opposite side of the open lid versus the spin label at position 181 (Figure 6B). Here again, it was surprising to observe only one distance corresponding to the open HPL whereas the sample also contained 35% HPL in the closed conformation, and two additional distances were expected in association with the two spin label conformational subensembles at position 249 of the closed HPL lid. We have seen previously that one of these distances (lower than 10 Å) is too small to be estimated by DEER experiments. The distance between the second spin label conformational subensemble at position 249 and that at position 181 was estimated to be 19 Å, and the interaction between these spin labels could therefore be detected by DEER (distances >15 Å). But the residual concentration of bilabeled and closed HPL corresponding to this situation was however estimated to be close to 7 μM, and it is not surprising that this contribution was not detected by DEER for sensitivity reasons.

In conclusion, EPR spectroscopy allowed the measurement of two distances corresponding to the closed and the open conformations of the HPL lid, respectively. The amplitude of the side chain displacement for residue 249 was estimated to be 24 Å, a value similar to that deduced from X-ray 3D structures of HPL (*10*). The DEER method is therefore a valuable tool for measuring the amplitude of the HPL lid opening in a frozen solution. The use of both CW and pulsed EPR spectroscopy, as well as the identification of spin label conformational subensembles, was however requested for interpreting correctly the results.

These experiments supported the existence of two spin label conformational subensembles at position 249 when HPL is in its closed conformation, these spin labels being separated from the spin label at position 181 by distances lower than 10 Å and equal to 19 Å, respectively. These values are compatible with the results of molecular dynamics and X-ray crystallography (Figures 5 and 6).

More importantly, the present findings confirmed the previous attribution of distinct EPR spectra to the closed (narrow-shaped) and open (broad-shaped) conformations of the HPL lid. This attribution was indirectly based on experiments performed with the E600 inhibitor bound to the active site and blocking HPL in the open conformation (*19*). The broad-shaped EPR spectrum of monolabeled HPL at position 249 was always recorded under the same conditions that allowed to measure the maximum amplitude of the lid opening with bilabeled HPL and DEER experiments: either by using bile salts and colipase (42 Å) or by lowering the pH to 4.5 (46 Å), this later condition also promoting the lid opening in HPL (*20*).

The previous work by Belle et al. allowed to quantify the equilibrium between the closed and the open conformation of HPL in solution and to establish that it was a reversible process (*19*). The present work allowed to quantify the lid opening process in solution and in frozen solution by measuring the displacement of one residue located within the lid. Although the distances estimated from EPR experiments are similar to those already deduced from X-ray crystallography, these previous results were obtained in a crystal structure. When various conformations of the lipase lid were observed for the first time, the question was raised whether these conformations could exist in solution or resulted from crystal packing constraints. The data presented here support the existence of HPL conformations in solution identical to those observed in the enzyme crystals. This is an important step forward in the understanding of HPL structure−function relationships under conditions closer to those found in the physiological environment of the enzyme. It is worth noticing that the enzyme concentration (micromolar) in the samples used for EPR experiments is in the same range as the mean HPL concentration measured in samples collected from the small intestine during a meal (250 μg/mL or 5 μM (*44*)).

The next step will consist of experiments performed with lipids to investigate the lid opening process when the HPL binds at a lipid−water interface. The existence of two spin label conformational subensembles with moderate mobility is the fingerprint of the lid in its closed conformation, and this property might be particularly useful for such a study.

ACKNOWLEDGMENT

We thank Dr. Robert Verger for fruitful discussions and continuous interest in this work. We are grateful to Dr. Janez Strancar (Laboratory of Biophysics, EPR Center, "Jozef Stefan" Institute, Ljubljana, Slovenia) for providing the EPRSIM-C software program for EPR spectrum simulation and to Dr. Jessica Blanc for revising the English manuscript.

REFERENCES

1. Carrière, F., Barrowman, J. A., Verger, R., and Laugier, R. (1993) Secretion and contribution to lipolysis of gastric and pancreatic lipases during a test meal in humans. *Gastroenterology 105*, 876–888.
2. Borgström, B., and Brockman, H. L. (1984) Lipases, pp 1−527, Elsevier, Amsterdam.
3. Schmid, R. D., and Verger, R. (1998) Lipases: interfacial enzymes with attractive applications. *Angew. Chem., Int. Ed. 37*, 1608–1633.
4. Wooley, P., and Petersen, S. B. (1994) Lipases: their structure, biochemistry and applications, pp 1−363, Cambridge University Press, Cambridge.
5. Aloulou, A., Rodriguez, J. A., Fernandez, S., Van Oosterhout, D., Puccinelli, D., and Carriere, F. (2006) Exploring the specific features of interfacial enzymology based on lipase studies. *Biochim. Biophys. Acta 1761*, 995–1013.
6. Brady, L., Brzozowski, A. M., Derewenda, Z. S., Dodson, E., Dodson, G., Tolley, S., Turkenburg, J. P., Christiansen, L., Huge-Jensen, B., Norskov, L., Thim, L., and Menge, U. (1990) A serine protease triad forms the catalytic centre of a triacylglycerol lipase. *Nature 343*, 767–770.
7. Winkler, F. K., d'Arcy, A., and Hunziker, W. (1990) Structure of human pancreatic lipase. *Nature 343*, 771–774.
8. Roussel, A., Canaan, S., Egloff, M. P., Riviere, M., Dupuis, L., Verger, R., and Cambillau, C. (1999) Crystal structure of human gastric lipase and model of lysosomal acid lipase, two lipolytic enzymes of medical interest. *J. Biol. Chem. 274*, 16995–17002.
9. Brzozowski, A. M., Derewenda, U., Derewenda, Z. S., Dodson, G. G., Lawson, D. M., Turkenburg, J. P., Bjorkling, F., Huge-Jensen, B., Patkar, S. A., and Thim, L. (1991) A model for interfacial activation in lipases from the structure of a fungal lipase-inhibitor complex. *Nature 351*, 491–494.
10. van Tilbeurgh, H., Egloff, M.-P., Martinez, C., Rugani, N., Verger, R., and Cambillau, C. (1993) Interfacial activation of the lipase-procolipase complex by mixed micelles revealed by X-ray crystallography. *Nature 362*, 814–820.
11. Roussel, A., Miled, N., Berti-Dupuis, L., Riviere, M., Spinelli, S., Berna, P., Gruber, V., Verger, R., and Cambillau, C. (2002) Crystal structure of the open form of dog gastric lipase in complex with a phosphonate inhibitor. *J. Biol. Chem. 277*, 2266–2274.
12. Egloff, M.-P., Marguet, F., Buono, G., Verger, R., Cambillau, C., and van Tilbeurgh, H. (1995) The 2.46 Å resolution structure of the pancreatic lipase-colipase complex inhibited by a C11 alkyl phosphonate. *Biochemistry 34*, 2751–2762.
13. Miled, N., Roussel, A., Bussetta, C., Berti-Dupuis, L., Riviere, M., Buono, G., Verger, R., Cambillau, C., and Canaan, S. (2003) Inhibition of dog and human gastric lipases by enantiomeric phosphonate inhibitors: a structure-activity study. *Biochemistry 42*, 11587–11593.
14. Hermoso, J., Pignol, D., Kerfelec, B., Crenon, I., Chapus, C., and Fontecilla-Camps, J. C. (1996) Lipase activation by nonionic detergents. The crystal structure of the porcine lipase-colipase-tetraethylene glycol monooctyl ether complex. *J. Biol. Chem. 271*, 18007–18016.
15. Hermoso, J., Pignol, D., Penel, S., Roth, M., Chapus, C., and Fontecilla-Camps, J. C. (1997) Neutron crystallographic evidence of lipase-colipase complex activation by a micelle. *EMBO J. 16*, 5531–5536.
16. Prompers, J. J., Groenewegen, A., Hilbers, C. W., and Pepermans, H. A. (1999) Backbone dynamics of *Fusarium solani pisi* cutinase probed by nuclear magnetic resonance: the lack of interfacial activation revisited. *Biochemistry 38*, 5315–5327.
17. Prompers, J. J., van Noorloos, B., Mannesse, M. L., Groenewegen, A., Egmond, M. R., Verheij, H. M., Hilbers, C. W., and Pepermans, H. A. (1999) NMR studies of *Fusarium solani pisi* cutinase in complex with phosphonate inhibitors. *Biochemistry 38*, 5982–5994.
18. Sibille, N., Favier, A., Azuaga, A. I., Ganshaw, G., Bott, R., Bonvin, A. M., Boelens, R., and van Nuland, N. A. (2006) Comparative NMR study on the impact of point mutations on protein stability of *Pseudomonas mendocina* lipase. *Protein Sci. 15*, 1915–1927.
19. Belle, V., Fournel, A., Woudstra, M., Ranaldi, S., Prieri, F., Thome, V., Currault, J., Verger, R., Guigliarelli, B., and Carriere, F. (2007) Probing the opening of the pancreatic lipase lid using site-directed spin labeling and EPR spectroscopy. *Biochemistry 46*, 2205–2214.
20. Ranaldi, S., Belle, V., Woudstra, M., Rodriguez, J., Guigliarelli, B., Sturgis, J., Carriere, F., and Fournel, A. (2009) Lid opening and unfolding in human pancreatic lipase at low pH revealed by site-directed spin labeling EPR and FTIR spectroscopy. *Biochemistry 48*, 630–638.
21. Thirstrup, K., Carriere, F., Hjorth, S., Rasmussen, P. B., Woldike, H., Nielsen, P. F., and Thim, L. (1993) One-step purification and characterization of human pancreatic lipase expressed in insect cells. *FEBS Lett. 327*, 79–84.
22. Jeschke, G. (2002) Distance measurements in the nanometer range by pulsed EPR. *ChemPhysChem 3*, 927–932.
23. Jeschke, G., Chechik, V., Godt, A., Zimmermann, H., Banham, J., Timmel, C. R., Hilger, D., and Jung, H. (2006) DEER analysis 2006—a computational software package for analyzing pulsed ELDOR data. *Appl. Magn. Reson. 30*, 473–498.

24. Tikhonov, A. N., and Arsenin, V. Y. (1977) Solutions of Ill-posed Problems, pp 1−272, John Wiley & Sons, New York.
25. Strancar, J., Koklic, T., Arsov, Z., Filipic, B., Stopar, D., and Hemminga, M. A. (2005) Spin label EPR-based characterization of biosystem complexity. *J. Chem. Inf. Model. 45*, 394–406.
26. Strancar, J. (2007) Advanced ESR spectrocopy in membrane biophysics, in ESR spectroscopy in membrane biophysics (Berliner, L. J., Ed.) pp 49−89, Springer, New York.
27. Morin, B., Bourhis, J. M., Belle, V., Woudstra, M., Carriere, F., Guigliarelli, B., Fournel, A., and Longhi, S. (2006) Assessing induced folding of an intrinsically disordered protein by site-directed spin-labeling electron paramagnetic resonance spectroscopy. *J. Phys. Chem. B 110*, 20596–20608.
28. Brooks, B. R., Brooks, C. L., III, Mackerell, A. D., Jr., Nilsson, L., Petrella, R. J., Roux, B., Won, Y., Archontis, G., Bartels, C., Boresch, S., Caflisch, A., Caves, L., Cui, Q., Dinner, A. R., Feig, M., Fischer, S., Gao, J., Hodoscek, M., Im, W., Kuczera, K., Lazaridis, T., Ma, J., Ovchinnikov, V., Paci, E., Pastor, R. W., Post, C. B., Pu, J. Z., Schaefer, M., Tidor, B., Venable, R. M., Woodcock, H. L., Wu, X., Yang, W., York, D. M., and Karplus, M. (2009) CHARMM: the biomolecular simulation program. *J. Comput. Chem. 30*, 1545–1614.
29. Sale, K., Song, L., Liu, Y. S., Perozo, E., and Fajer, P. (2005) Explicit treatment of spin labels in modeling of distance constraints from dipolar EPR and DEER. *J. Am. Chem. Soc. 127*, 9334–9335.
30. Sale, K., Sar, C., Sharp, K. A., Hideg, K., and Fajer, P. G. (2002) Structural determination of spin label immobilization and orientation: a Monte Carlo minimization approach. *J. Magn. Reson. 156*, 104–112.
31. Guo, Z., Cascio, D., Hideg, K., and Hubbell, W. L. (2008) Structural determinants of nitroxide motion in spin-labeled proteins: solvent-exposed sites in helix B of T4 lysozyme. *Protein Sci. 17*, 228–239.
32. Ryckaert, J. P., Ciccotti, G., and Berendsen, H. J. C. (1977) Numerical integration of the cartesian equations of motion of a system with constraints: molecular dynamics of n-alkanes. *J. Comput. Phys. 23*, 327–341.
33. van Tilbeurgh, H., Sarda, L., Verger, R., and Cambillau, C. (1992) Structure of the pancreatic lipase-procolipase complex. *Nature 359*, 159–162.
34. Brzozowski, A. M., Savage, H., Verma, C. S., Turkenburg, J. P., Lawson, D. M., Svendsen, A., and Patkar, S. (2000) Structural origins of the interfacial activation in *Thermomyces* (*Humicola*) *lanuginosa* lipase. *Biochemistry 39*, 15071–15082.
35. Lovell, S. C., Word, J. M., Richardson, J. S., and Richardson, D. C. (2000) The penultimate rotamer library. *Proteins 40*, 389–408.
36. Beier, C., and Steinhoff, H. J. (2006) A structure-based simulation approach for electron paramagnetic resonance spectra using molecular and stochastic dynamics simulations. *Biophys. J. 91*, 2647–2664.
37. Sezer, D., Freed, J. H., and Roux, B. (2008) Using Markov models to simulate electron spin resonance spectra from molecular dynamics trajectories. *J. Phys. Chem. B 112*, 11014–11027.
38. Caves, L. S., Evanseck, J. D., and Karplus, M. (1998) Using Markov models to simulate electron spin resonance spectra from molecular dynamics trajectories. *Protein Sci. 7*, 649–666.
39. Buck, M., Bouguet-Bonnet, S., Pastor, R. W., and MacKerell, A. D., Jr. (2006) Importance of the CMAP correction to the CHARMM22 protein force field: dynamics of hen lysozyme. *Biophys. J. 90*, L36–38.
40. Langen, R., Oh, K. J., Cascio, D., and Hubbell, W. L. (2000) Crystal structures of spin labeled T4 lysozyme mutants: implications for the interpretation of EPR spectra in terms of structure. *Biochemistry 39*, 8396–8405.
41. Guo, Z., Cascio, D., Hideg, K., Kalai, T., and Hubbell, W. L. (2007) Structural determinants of nitroxide motion in spin-labeled proteins: tertiary contact and solvent-inaccessible sites in helix G of T4 lysozyme. *Protein Sci. 16*, 1069–1086.
42. Fleissner, M. R., Cascio, D., and Hubbell, W. L. (2009) Structural origin of weakly ordered nitroxide motion in spin-labeled proteins. *Protein Sci. 18*, 893–908.
43. Pistolesi, S., Ferro, E., Santucci, A., Basosi, R., Trabalzini, L., and Pogni, R. (2006) Molecular motion of spin labeled side chains in the C-terminal domain of RGL2 protein: a SDSL-EPR and MD study. *Biophys. Chem. 123*, 49–57.
44. Carriere, F., Renou, C., Lopez, V., De Caro, J., Ferrato, F., Lengsfeld, H., De Caro, A., Laugier, R., and Verger, R. (2000) The specific activities of human digestive lipases measured from the in vivo and in vitro lipolysis of test meals. *Gastroenterology 119*, 949–960.